Correction of Deafness in *shaker-2* Mice by an Unconventional Myosin in a BAC Transgene

Frank J. Probst, Robert A. Fridell, Yehoash Raphael, Thomas L. Saunders, Aihui Wang, Yong Liang, Robert J. Morell, Jeffrey W. Touchman, Robert H. Lyons, Konrad Noben-Trauth, Thomas B. Friedman, Sally A. Camper*

The *shaker-2* mouse mutation, the homolog of human *DFNB3*, causes deafness and circling behavior. A bacterial artificial chromosome (BAC) transgene from the *shaker-2* critical region corrected the vestibular defects, deafness, and inner ear morphology of *shaker-2* mice. An unconventional myosin gene, *Myo15*, was discovered by DNA sequencing of this BAC. *Shaker-2* mice were found to have an amino acid substitution at a highly conserved position within the motor domain of this myosin. Auditory hair cells of *shaker-2* mice have very short stereocilia and a long actin-containing protrusion extending from their basal end. This histopathology suggests that *Myo15* is necessary for actin organization in the hair cells of the cochlea.

Shaker-2 (*sh2*) is a recessive mouse mutation on chromosome 11 that arose in the progeny of an x-ray–irradiated mouse (*1*) and has been proposed as the mouse model of *DFNB3* (*2*). Affected mice lack the normal startle response to sound and show no auditory brainstem responses to sound pressure levels up to 90 dB SPL at frequencies of 4, 10, and 20 kHz, indicating profound deafness (*3*). Associated vestibular defects cause head-tossing and circling behavior (Fig. 1A).

The stereociliary bundles on both the inner and outer hair cells of 1-month-old *shaker-2* mice are dysmorphic (Fig. 1). The stereocilia are extremely short, but scanning electron microscopy shows that they are arrayed in a nearly normal pattern. Whole mounts of the organ of Corti stained with phalloidin reveal a long actin-containing structure associated with mutant inner hair cells. Visualization of actin staining in the mutant mice by scanning laser confocal microscopy demonstrates that the prominent actin bundle is initiated beneath the cuticular plate of the inner hair cells, continues in a basal direction, and extends from the base of each cell in a medial orientation for up to 50 μm. The presence of this abnormal actin-containing structure on inner hair cells suggests that the *sh2* gene is critical for normal cytoskeletal morphology and actin organization. Other loci for genetic deafness share this phenotypic feature with *shaker-2* (*4*). These loci may represent defects in different steps of a common pathway or different components of a multisubunit actin-organizing system.

Recently, fine genetic mapping placed *sh2* in a region of chromosome 11 near four

F. J. Probst, T. L. Saunders, S. A. Camper, Department of Human Genetics, 4701 MSRB III, University of Michigan, 1500 West Medical Center Drive, Ann Arbor, MI 48109, USA.
R. A. Fridell, R. J. Morell, K. Noben-Trauth, T. B. Friedman, National Institute on Deafness and Other Communication Disorders (NIDCD), National Institutes of Health, 5 Research Court, Rockville, MD 20850, USA.
A. Wang and Y. Liang, Graduate Program in Genetics, Michigan State University, East Lansing, MI 48824, USA, and NIDCD, 5 Research Court, Rockville, MD 20850, USA.
Y. Raphael, Kresge Hearing Research Institute, University of Michigan, Ann Arbor, MI 48109, USA.
J. W. Touchman, NIH Intramural Sequencing Center, 5 Research Court, Rockville, MD 20850, USA, and National Human Genome Research Institute, 49 Convent Drive, Room 2C36, Bethesda, MD 20892, USA.
R. H. Lyons, DNA Sequencing Core Facility, University of Michigan, Ann Arbor, MI 48109, USA.
*To whom correspondence should be addressed. E-mail: scamper@umich.edu

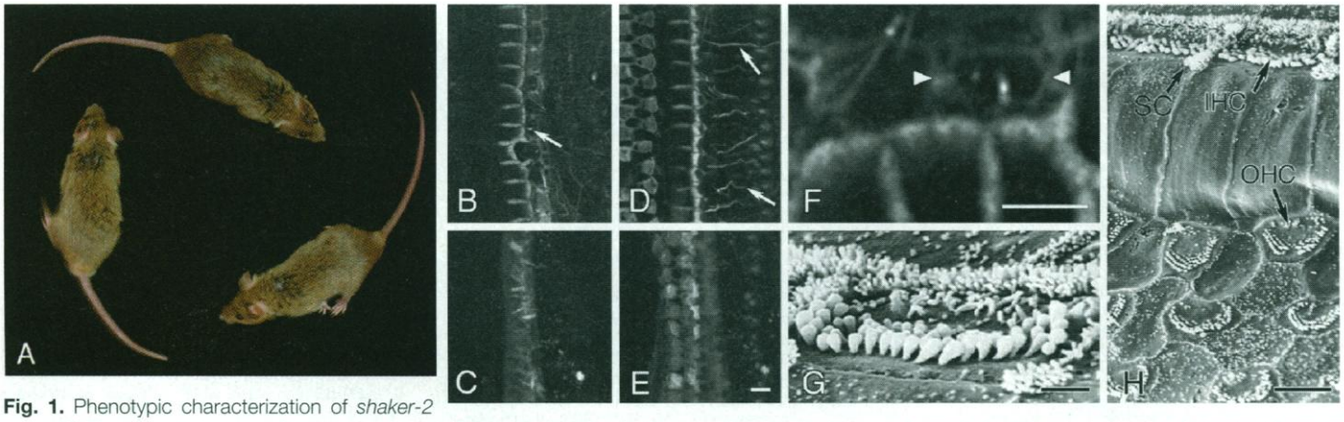

Fig. 1. Phenotypic characterization of *shaker-2* mice. (**A**) Time-lapse photography captures the circling behavior of a single *shaker-2* homozygote. (**B** to **E**) Whole mounts of organ of Corti from 1-month-old normal and mutant mice were stained with rhodamine-conjugated phalloidin to visualize actin and analyzed by laser scanning confocal microscopy (*17*). In all cases, normal controls were wild-type littermates of affected mice. Micrographs are oriented with the outer hair cells at the left and inner hair cells at the right. Panels (B) and (C) represent a focal plane immediately beneath the cuticular plate (adjacent to the luminal surface of the epithelium); (D) and (E) are optical sections at a focal plane near the basal end of inner hair cells (close to the basal lamina). In (B), laser scanning confocal microscopy of the inner hair cells shows an actin-rich area in the center of each cell (arrow), which was absent in wild-type mice (C). In the mutants (D), each inner hair cell was associated with one long abnormal actin-containing structure that projected from the base of the cell (arrows); normal mice lacked this structure (E). Scale bar, 10 μm. (**F**) High-magnification laser scanning confocal optical section through the subapical domain of a mutant inner hair cell. Micrograph is oriented with inner hair cells at the top. The apical borders of the inner hair cell are identified by junction-associated actin, in contact with two flanking supporting cells (arrowheads), as well as junctions with supporting cells at medial and lateral aspects. The abnormal actin-containing structure was clearly viewed in the center of the inner hair cell. Scale bar, 10 μm. (**G**) Cochlea prepared for scanning electron microscopy (*17*) revealed the apical (luminal) surface of an inner hair cell in a 1-month-old *sh2*/*sh2* mouse. Stereocilia were extremely short, and some were located away from the normal bundle site. Scale bar, 2 μm. (**H**) Scanning electron microscopy of a 1-month-old mutant mouse cochlea showing two inner hair cells (IHC labels the cell on the right), a supporting cell (SC) positioned between the two inner hair cells, and the three rows of outer hair cells (OHC identifies a first-row cell). Stereocilia of outer hair cells were extremely short. Several stereocilia on each outer hair cell were located outside the typical bundle location.

genes whose homologs map to 17p11.2 in the critical region for a human recessive congenital deafness, *DFNB3* (3). Complete 1-Mb yeast artificial chromosome and BAC contigs that span the *shaker-2* critical region have been generated (5). Because there were no compelling candidate genes in the nonrecombinant region, we adopted an in vivo complementation approach to narrow the *sh2* critical region. BAC clones from the contig were injected individually into fertilized eggs from *sh2/sh2* parents, and a BAC clone that rescues the *sh2* phenotype was identified. A transgenic founder that responded to sound and did not circle was shown to contain the BAC 425p24 clone. This founder was mated to a *sh2/sh2* female, and four of six progeny had normal hearing and behavior. Only the animals that inherited the transgene exhibited correction of the *shaker-2* phenotype. The hair cells of a *sh2/sh2* animal rescued by the BAC transgene had normal stereocilia (Fig. 2) and no unusual actin-containing structures. This confirmed that BAC 425p24 contains the *sh2* gene and sufficient regulatory sequences for phenotypic correction.

To identify the *shaker-2* gene, we sequenced the 140-kb BAC 425p24 and examined it for potential coding regions, using GENSCAN, GRAIL, and BLAST (6). This approach identified a gene encoding a novel unconventional myosin that we have designated *Myo15*. Partial *Myo15* cDNAs were isolated by polymerase chain reaction (PCR) amplification from an embryonic day 17 (E17) mouse cDNA library using primers derived from predicted exons of *Myo15*. To date, a deduced 5352–base pair (bp) cDNA spanning 49 exons has been assembled. This cDNA contains an open reading frame throughout its length and is predicted to encode a 1783–amino acid peptide of >200 kD. Northern (RNA) blot analysis detects a ~5-kb transcript in adult mouse brain and kidney (Fig. 3A), suggesting that the current cDNA is nearly full-length. Reverse transcription PCR (RT-PCR) analysis reveals that *Myo15* is expressed in the inner ear of E18 mouse embryos as well as in adult brain and liver (Fig. 3B).

Myosins are mechanoenzymes that bind F-actin and hydrolyze adenosine triphosphate (ATP) to produce force. These proteins are involved in diverse functions including vesicle movement, extension of cellular processes, cytokinesis, phagocytosis, signal transduction, cellular movement, and muscle contraction. Features common to all myosins are a conserved motor domain responsible for its actin-activated adenosine triphosphatase (ATPase) activity, regulatory domains that bind light chains such as calmodulin, and various dissimilar tail structures that may be involved in binding membranes, cargo, or both (7). Comparison with other myosins indicates that the motor domain of Myo15 extends from amino acids 41 to 714 and includes a consensus ATP binding site and a potential ATP–guanosine triphosphate (GTP) binding site (8). The COOH-terminal region of Myo15 has several interesting features, including similarities to the talin and myosin tail (MyTH4) domains [for details, see (9)].

Myosins are divided into subclasses on the basis of comparisons of the motor domains and features of the tail. Conventional myosins constitute class II, and the other 13 classes are unconventional myosins. A genetic distance tree was constructed with a portion of the motor domains of 40 myosins, including each of the known classes as well as *Myo15* and its human homolog, *MYO15*. Neither *Myo15* nor *MYO15* joined any of the existing branches of the unrooted tree with greater than 50% confidence, which suggests that these genes are sufficiently divergent to constitute a new class designated myosin-XV (Fig. 4A).

No obvious rearrangements, insertions, or deletions were detected in the *Myo15* gene (10), which suggested that a point mutation was the likely cause of the *shaker-2* defect. PCR primers were designed to amplify all 49 of the exons identified in cDNAs or predicted by one of the gene identification algorithms. In general, 20 to 100 bp of flanking intronic sequence were included in the amplification products. In codon 674 within exon 18, a G → A transition was found that produces a Cys → Tyr substitution (Fig. 4B). The presence of this alteration was confirmed by restriction digestion of PCR-amplified genomic DNA from *sh2* homozygotes and heterozygotes (Fig. 4C). This is a highly conserved amino acid within the motor domain, with 78 of 82 myosins examined containing a cysteine residue at the corresponding position (11). The genes that do not encode Cys at this

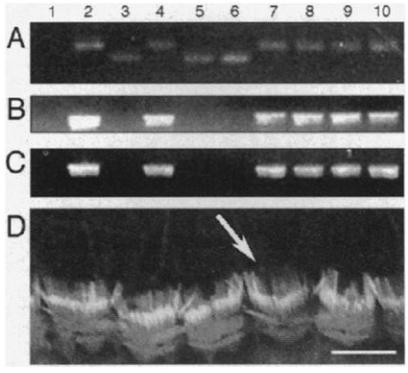

Fig. 2. Transgene correction of *shaker-2*. BAC 425p24 was obtained from Research Genetics after screening of their 129/Sv mouse BAC library with the polymorphic marker *D11Mit26* (18). The ends of the BAC were sequenced directly using Sp6 and T7 primers. Primers were designed to amplify the vector-insert junctions of the BAC (forward: Sp6 primer, reverse: 5′-CCTCAACCTCTGTGGGTTGT-3′; forward: T7 primer, reverse: 5′-CTGTCGAGTTGGCTCATTGA-3′). Fertilized eggs collected from *sh2/sh2* females mated with *sh2/sh2* males were injected with BAC 425p24 miniprep DNA that had been digested with Not I and dialyzed against microinjection buffer. A total of 51 eggs were injected and eight pups were born (19). All pups were typed for (**A**) *D11Mit26* and the unique vector insert junctions at the (**B**) Sp6 end and (**C**) T7 ends of the BAC. Controls are water (lane 1), BAC 425p24 (lane 2), and *sh2/sh2* (lane 3). One mouse had normal behavior and a startle response to sound (lane 4). Only this mouse had the 129/Sv allele of *D11Mit26* from the BAC and scored positive for the BAC vector-insert junctions. This founder was mated to a *sh2/sh2* female. Scoring of the progeny for BAC-specific PCR products demonstrated cosegregation of the transgene with restoration of hearing (lanes 7 to 10), whereas nontransgenic animals were deaf and exhibited head-tossing and circling behavior (lanes 5 and 6). (**D**) The presence of normal stereocilia on inner hair cells (arrow) in a 2-month-old progeny of the transgenic founder were demonstrated by analysis of the organ of Corti by laser scanning confocal microscopy. Scale bar, 10 μm.

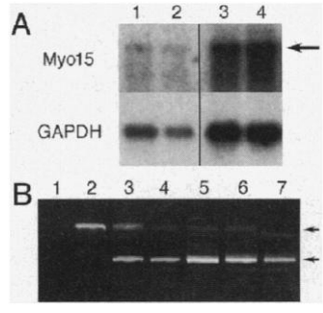

Fig. 3. *Myo15* is expressed in the inner ear. (**A**) Northern blot analysis reveals expression of *Myo15* in adult brain (lanes 1 and 2) and kidney (lanes 3 and 4). A blot containing 2 μg of poly-A$^+$ RNA from adult brains and kidneys of normal (lanes 1 and 3) and *sh2* mutant (lanes 2 and 4) mice was hybridized with two antisense riboprobes that together correspond to the COOH-terminal 1351 nucleotides of the *Myo15* cDNA (exons 40 to 48). The blot was washed to a final stringency of 0.1× SSC at 68°C and exposed for 9 hours with two intensifying screens. A primary hybridizing band of ~5 kb was noted in both tissues (arrow). The blot was subsequently stripped and reprobed with a GAPDH probe (exposure 5 hours). (**B**) RT-PCR was used to detect *Myo15* transcripts in 1 μg of total RNA from adult mouse liver (lane 3), brain (lane 4), and three different preparations of E18 mouse inner ear (lanes 5 to 7). Controls were water (lane 1) and mouse genomic DNA (lane 2). Primers used for PCR amplification were derived from *Myo15* exons 34 to 38. The 760- and 450-bp products (arrows) correspond to the sizes expected from amplification of *Myo15* genomic DNA and cDNA, respectively. DNA sequencing confirmed that the 450-bp RT-PCR product was a *Myo15* cDNA fragment.

position have conservative changes to Thr or Leu. The substitution of a hydrophobic Tyr residue is likely to disrupt the function of the myosin motor (Fig. 4D). This cysteine is within a putative actin binding site. Substitution of Arg-Cys-Ile in the comparable region of the *Drosophila* class III myosin, *Nina*C, with Leu-Phe-Asn results in a null allele (*12*). Thus, the *shaker-2* muta-

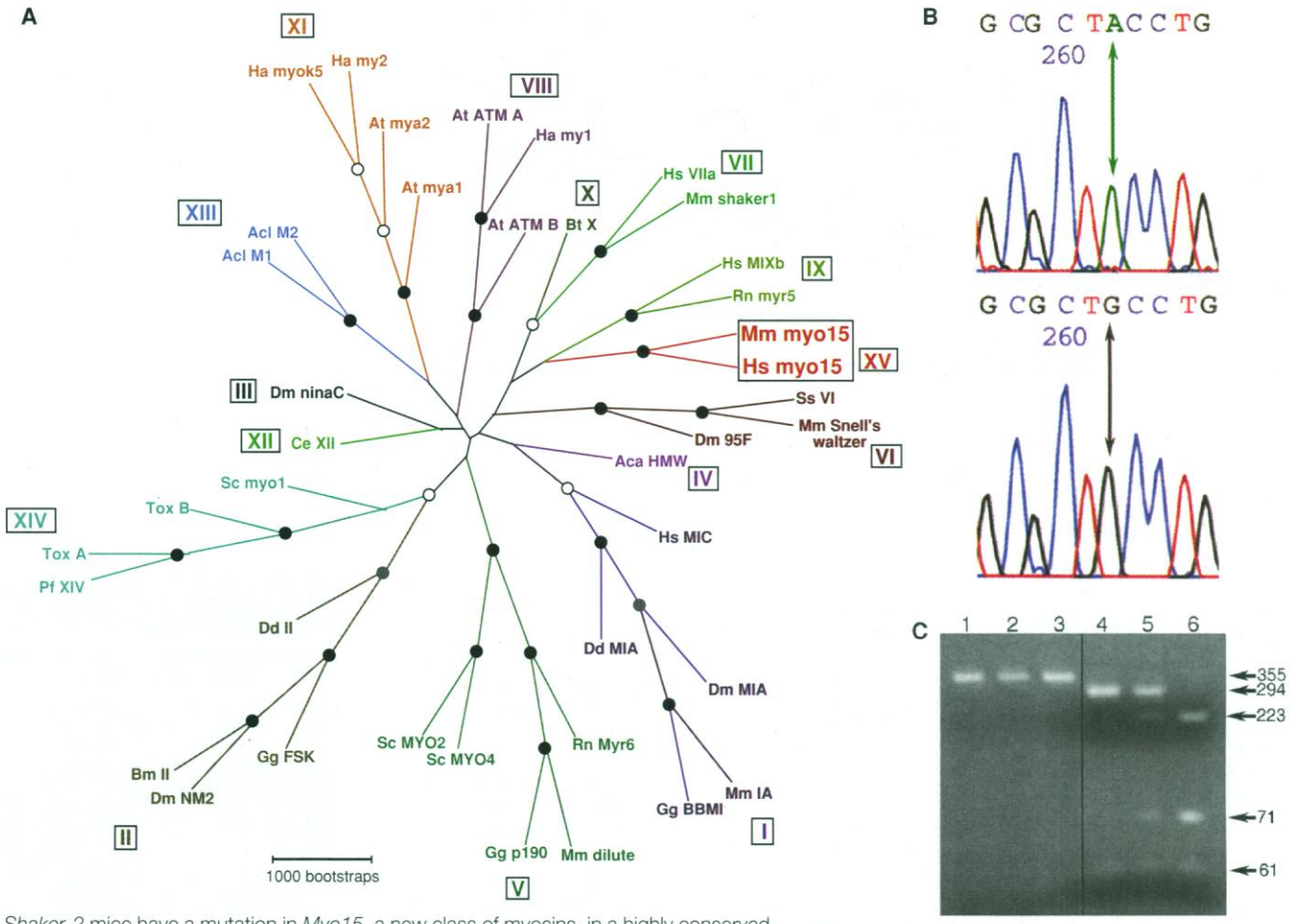

D

	Mm Myo15 (sh2/sh2)	P	L	F	V	R	Y	L	K	P	N	H	K
	Mm Myo15 (+/+)	P	L	F	V	R	C	L	K	P	N	H	K
	Hs MYO15	P	L	F	M	R	C	L	K	P	N	H	K
I	*DdIA*	P	H	Y	V	R	C	I	K	P	N	S	N
II	*ScMyoI (IIA)*	P	H	F	V	R	C	I	I	P	N	N	V
III	*Dm NinaC*	V	H	F	V	R	C	I	R	A	D	L	E
IV	*Ac HMWM1*	P	H	Y	I	R	C	T	K	P	N	S	E
V	*Mm dilute*	P	H	Y	V	R	C	I	K	P	N	D	F
VI	*Mm Myo VI (sv)*	A	S	F	I	R	C	I	K	P	N	L	K
VII	*Mm MyoVII (sh1)*	P	F	F	V	R	C	I	K	P	N	E	F
VIII	*At ATM (VIIIB)*	P	H	F	I	R	C	I	K	P	N	S	K
IX	*Rnmyr5*	P	F	F	I	R	C	I	R	S	N	A	E
X	*Bt X*	P	F	F	V	R	C	I	K	P	N	M	Q
XI	*At MYA2 (XIB)*	P	H	Y	I	R	C	V	K	P	N	N	L

Fig. 4. *Shaker-2* mice have a mutation in *Myo15*, a new class of myosins, in a highly conserved amino acid. (**A**) An unrooted genetic distance tree illustrates the divergence of *Myo15* from other classes of myosins (*20*). Forty myosin proteins from the public databases were aligned with ClustalW using the default settings. The portion selected represented amino acids 213 to 511 in chicken fast skeletal muscle myosin (GgFsk), a class II conventional myosin. The PHYLIP package of programs was used to generate a genetic distance tree; 1000 bootstrap data sets were generated and analyzed with the programs PROTDIST and NEIGHBOR, and the program CONSENSE produced the unrooted tree. Nodes appearing in >90%, >70%, or >50% of the bootstrap trials are denoted by solid circles, gray circles, and open circles, respectively. The species represented are *Acanthamoeba castellanii* (Aca), *Acetabularia cliftonii* (Acl), *Arabidopsis thaliana* (At), *Brugia malayi* (Bm), *Bos taurus* (Bt), *Dictyostelium discoidium* (Dd), *Drosophila melanogaster* (Dm), *Gallus gallus* (Gg), *Helianthus annus* (Ha), *Homo sapiens* (Hs), *Mus musculus* (Mm), *Plasmodium falciparum* (Pf), *Rattus norvegicus* (Rn), *Saccharomyces cerevisiae* (Sc), *Schistosoma mansoni* (Sm); *Sus scrofa* (Ss), and *Toxoplasma gondii* (Tox). The accession numbers for the sequences, by class, are as follows: **class I:** MmIA L00923, Gg BBM I U04049, Dm MIA S45573, Dd MIA P22467, Hs MIC U14391; **class II:** BmII M74000, Dm NM2 P05661, Gg Fsk P13538, DdII p08799; Sc myo1 (IIA) S46773; **class III:** Dm Nina C p10676; **class IV:** Aca HMW j05678; **class V:** Mm dilute V x57377, Gg p190 z11718, Rn myr6 u60416, Sc Myo2(VA) p19524, Sc myo4(VB) p32492; **class VI:** Mm *Snell's waltzer* u49739, Ss VI a54818, Dm 95F Q01989; **class VII:** Mm *shaker-1* U81453, Hs VIIa u55208; **class VIII:** At ATM A x67104, At ATM B z34292, Ha my 1 U94781; **class IX:** Rn myr5 x77609, Hs MIXb u42391; **class X:** BtX U55042; **class XI:** At mya2 z34294, At mya1 z28389, Ha myok5 U94785, Ha my2 U94782; **class XII:** Ce XII z66563; **class XIII:** Acl M2 U94398, Acl M1 U94397; **class XIV:** Tox A af006626, Pf XIV y09693, ToxB af006627. (**B**) DNA sequence of exon 18 from *sh2/sh2* (top) and C57BL/6J (bottom) mice revealed a G → A transition that results in a Cys → Tyr change. (**C**) This change disrupts a restriction site for Tse I (GCWGC). Genomic DNA from *sh2/sh2* (lanes 1 and 4) and *sh2*/+ (lanes 2 and 5) mice and DNA from BAC 425p24 (lanes 3 and 6) were amplified (forward primer: 5′-GTAGCACACCTTTTCTCCAG-3′; reverse primer: 5′-AGTGCCACACTTCA-CAGG-3′) by PCR. Products were not digested (lanes 1 to 3) or digested with Tse I (lanes 4 to 6), separated by gel electrophoresis, and stained with ethidium bromide. The BAC 425p24 product gives bands at 223, 71, and 61 bp, as there are two Tse I sites in the PCR product. *sh2/sh2* mice are homozygous for the disruption of one of these two sites and thus have only 294- and 61-bp bands. *sh2*/+ mice are heterozygous for the change, as evidenced by the two banding patterns superimposed on one another. (**D**) The Cys → Tyr change occurs at a highly conserved position of the motor domain of this myosin. A ClustalW alignment of a 12–amino acid region from members of several myosin subclasses illustrates the location of the cysteine within a highly conserved sequence, PHFVRCIKPN (*16*), that has been proposed as part of an actin-binding region of the motor domain.

tion is likely to destroy actin binding of *Myo15*, creating a loss-of-function allele. *Myo15* led to identification of the human homolog, *MYO15*, and to the discovery of a nonsense mutation and two missense mutations in three unrelated human families with nonsyndromic, congenital deafness, *DFNB3* (9).

Mutations in three different unconventional myosins, $Myo15^{sh2}$, $Myo6^{sv}$, and $Myo7a^{sh1}$, cause deafness (13). Morphology and histology of severe loss-of-function alleles in the mouse suggest that each of these myosins has a unique function in the hair cells of the inner ear. Our results show that *Myo15* is involved in the maintenance of actin organization in the hair cells of the organ of Corti. Loss of *Myo7a* causes disorganization of the characteristic pattern of the stereocilia early in development, whereas loss of *Myo6* function causes fusion of the stereocilia and loss of the inner hair cells and support cells by 6 weeks of age (14). In contrast, the inner hair cells of *sh2* mutants survive longer (15) and the abnormally short stereocilia are arranged in a nearly normal pattern on the hair cell surface. These features make *shaker-2* mice a good model for examining the role of a unique unconventional myosin in the auditory system and for the exploration of mechanisms for the delivery of functional proteins to surviving mutant hair cells.

REFERENCES AND NOTES

1. N. Dobrovolskaia-Zavasdkaia, *Arch. Biol.* **38**, 457 (1928); G. D. Snell and L. W. Law, *J. Hered.* **30**, 447 (1939).
2. T. B. Friedman *et al.*, *Nature Genet.* **9**, 86 (1995).
3. Y. Liang *et al.*, *Am. J. Hum. Genet.* **62**, 904 (1998).
4. A. Sobin and A. Flock, *Adv. Oto-Rhino-Laryngol.* **25**, 12 (1981); D. Kohrman, E. Lambert, D. V. Garrett, D. F. Dolan, Y. Raphael, paper presented at the 21st Midwinter Research Meeting of the Association for Research in Otolaryngology, St. Petersburg Beach, FL, 1998 (www.aro.org); A. Sobin, M. Anniko, A. Flock, *Arch. Oto-Rhino-Laryngol.* **236**, 1 (1982).
5. Y. Wakabayashi *et al.*, *Biochem. Biophys. Res. Commun.* **234**, 107 (1997); F. Probst, Q. Xhao, K.-S. Chen, A. Wang, T. Friedman, J. Lupski, S. Camper, unpublished data.
6. R. K. Wilson and E. R. Mardis, in *Analyzing DNA*, B. Birren, E. D. Green, S. Klapholz, R. M. Myers, J. Roskams, Eds. (Cold Spring Harbor Laboratory Press, Cold Spring Harbor, NY, 1997), p. 398; S. F. Altschul, W. Gish, W. Miller, E. W. Myers, D. J. Lipman, *J. Mol. Biol.* **215**, 403 (1990). SeqWright Inc. (Houston, TX) generated the M13 DNA shotgun library and approximately half of the sequence data. Sequence contig assembly and editing were performed with the Sequencher program (Gene Codes Corp., Ann Arbor, MI); the web sites for GRAIL and GENSCAN are http://compbio.ornl.gov/Grail-bin/EmptyGrailForm and http://gnomic.stanford.edu/~chris/GENSCANW.html [C. Burge and S. Karlin, *J. Mol. Biol.* **268**, 78 (1997)].
7. V. Mermall, P. L. Post, M. S. Mooseker, *Science* **279**, 527 (1998).
8. P. Linder, *Nature* **337**, 121 (1989); the consensus ATP-GTP binding site is (A/G)XXXXGK(S/T/G) and the *Myo15* sequences are GESDSGKT, amino acids 132 to 139, and APPRLGKS at amino acids 566 to 573 (16). The *Myo15* cDNA sequence has been deposited in GenBank (accession number AF053130).
9. A. Wang *et al.*, *Science* **280**, 1447 (1998).
10. F. J. Probst, R. A. Fridell, Y. Raphael, T. L. Saunders, A. Wang, Y. Liang, R. J. Morell, J. W. Touchman, R. H. Lyons, K. Noben-Trauth, T. B. Friedman, S. A. Camper, data not shown.
11. Myosin home page, Medical Research Council, UK (www.mrc-lmb.cam.ac.uk/myosin/myosin.html).
12. H. M. Warrick and J. A. Spudich, *Annu. Rev. Cell. Biol.* **3**, 379 (1987); J. A. Porter and C. Montell, *J. Cell Biol.* **122**, 601 (1993).
13. K. A. Avraham *et al.*, *Nature Genet.* **11**, 369 (1995); F. Gibson *et al.*, *Nature* **374**, 62 (1995); D. Weil *et al.*, *ibid.*, p. 60; X. Liu *et al.*, *Nature Genet.* **16**, 188 (1997); D. Weil *et al.*, *ibid.*, p. 191; C. Petit, *ibid.* **14**, 385 (1996).
14. T. Self *et al.*, *Development* **125**, 557 (1998); K. Steel and K. Avraham, personal communication.
15. M. S. Deol, *J. Genet.* **52**, 562 (1954).
16. Abbreviations for the amino acid residues are as follows: A, Ala; C, Cys; D, Asp; E, Glu; F, Phe; G, Gly; H, His; I, Ile; K, Lys; L, Leu; M, Met; N, Asn; P, Pro; Q, Gln; R, Arg; S, Ser; T, Thr; V, Val; W, Trp; and Y, Tyr.
17. Y. Raphael and R. A. Altschuler, *Cell Motil. Cytoskeleton* **18**, 215 (1991); Y. Raphael, B. Athey, Y. Wang, M. K. Lee, R. A. Altschuler, *Hear. Res.* **76**, 173 (1994).
18. W. F. Dietrich *et al.*, *Nature Genet.* **7**, 220 (1994).
19. B. Hogan, R. Beddington, F. Costantini, E. Lacey, *Manipulating the Mouse Embryo: A Laboratory Manual* (Cold Spring Harbor Laboratory Press, Cold Spring Harbor, NY, 1994).
20. J. D. Thompson, D. G. Higgins, T. J. Gibson, *Nucleic Acids Res.* **22**, 4673 (1994); PHYLIP package, J. Felsenstein, University of Washington.
21. All experiments involving animals were approved by the University of Michigan Committee on the Use and Care of Animals. Animals were housed in facilities accredited by the American Association for the Accreditation of Laboratory Animal Care. The university's Animal Welfare Assurance is on file with the NIH Office for Protection from Research Risks (A3114-01). All procedures are in compliance with guidelines and standards set by local, state, and federal agencies.

Supported by NIDCD intramural research projects Z01 DC 00035, Z01 DC 00038, and Z01 DC 02407 (T.B.F.), and extramural grant R01DC 01634 (Y.R.), National Institute of Child Health and Human Development grant R01 HD30428 (S.A.C.), NSF (F.J.P.), and National Institute of General Medical Sciences grant T32 GM07863 (F.J.P.). We thank N. Dietrich, M. Fergusson, A. Gupta, E. Sorbello, R. Torkzadeh, C. Varner, M. Walker, G. Bouffard, and S. Beckstrom-Sternberg of the NIH Intramural Sequencing Center; C. Esposito, S. Genik, A. Thomas, and H. Luderer of the University of Michigan DNA Sequencing Core; P. Gillespie and M. Berard of the University of Michigan Transgenic Animal Model Core; L. Beyer, D. Dolan, K. Douglas, C. Edwards, E. Lambert, G. Levy, and P. Tucker of the University of Michigan; and J. Beals of PhotoGraphic for their contributions.

9 March 1998; accepted 17 April 1998

Association of Unconventional Myosin *MYO15* Mutations with Human Nonsyndromic Deafness *DFNB3*

Aihui Wang, Yong Liang, Robert A. Fridell, Frank J. Probst, Edward R. Wilcox, Jeffrey W. Touchman, Cynthia C. Morton, Robert J. Morell, Konrad Noben-Trauth, Sally A. Camper, Thomas B. Friedman*

DFNB3, a locus for nonsyndromic sensorineural recessive deafness, maps to a 3-centimorgan interval on human chromosome 17p11.2, a region that shows conserved synteny with mouse *shaker-2*. A human unconventional myosin gene, *MYO15*, was identified by combining functional and positional cloning approaches in searching for *shaker-2* and *DFNB3*. *MYO15* has at least 50 exons spanning 36 kilobases. Sequence analyses of these exons in affected individuals from three unrelated *DFNB3* families revealed two missense mutations and one nonsense mutation that cosegregated with congenital recessive deafness.

Nonsyndromic recessive deafness accounts for about 80% of hereditary hearing loss (1). To date, 20 loci responsible for this form of deafness have been mapped and three have been identified (2–4). *DFNB3*, first identified in families from Bengkala, Bali, initially was mapped to a 12-centimorgan (cM) region near the centromere of chromosome 17 (5) and subsequently was refined to a 3-cM region of 17p11.2 (6). Congenital hereditary deafness in two unrelated consanguineous families from India is also linked to *DFNB3* (6), indicating that the contribution of *DFNB3* alleles to hereditary deafness is likely to be geographically widespread.

On the basis of conserved synteny and similar phenotypes, we proposed that the autosomal recessive mouse mutation *shaker-2* was the homolog of *DFNB3* (5, 6). In the accompanying paper, we describe the bacterial artificial chromosome (BAC)–mediated transgene correction of the deafness and circling phenotype of homozygous *shaker-2* mice (7). DNA sequence analyses of this BAC revealed an unconventional myosin gene, *Myo15*. Myosins are a family of actin-based molecular motors that use energy from hydrolysis of adenosine triphosphate (ATP) to generate mechanical force. The classic, two-headed filament-forming myosins that provide the basis for muscle contraction are referred to as conventional myosins. Other members of the myosin superfamily, the unconventional myosins,